Temperature dependence of the thermoelectric effect of ion-bombarded NbN films: Evidence for the suppression of phonon drag and for renormalization

Th. Siebold and P. Ziemann
Fakultät für Physik, Universität Konstanz, D-78434 Konstanz, Germany
(Received 19 September 1994; revised manuscript received 8 November 1994)

The temperature dependence of the thermopower $S(T)$ of NbN_x films with different stoichiometry coefficients $x \geq 0.84$ has been experimentally determined within the range $4.2 \leq T \leq 300$ K. Within this temperature window, films with $x \geq 0.86$ exhibit positive S values with a broad peak centered at about 110 K and a nearly linear behavior for $T > 200$ K with a negative slope. For smaller x, the $S(T)$ curves are systematically depressed leading to a crossover from positive to negative values of the linear part at temperatures between 200 and 300 K. This shape of $S(T)$ could be explained by a superposition of a linear diffusion thermopower with negative slope, a phonon-drag part dominated by Umklapp processes and, at higher temperatures, a positive offset. Despite the high electrical resistivity of the films (> 300 $\mu\Omega$ cm), which is caused by grain-boundary scattering, the phonon-drag effect is not suppressed since the estimated phonon mean free path l_{ph} is still of the order of the grain size. By bombarding the films with increasing fluences of 350-keV Ne^+ ions, defects can be produced in the interior of the grains thereby systematically reducing l_{ph} resulting in a suppression of the phonon-drag peak as well as of the offset. For ion fluences corresponding to more than approximately one displacement per target atom (dpa), the ion-induced resistivity changes saturate at increases of typical 5% accompanied by a relative decrease of the superconducting transition temperatures of 14%. Due to the ion-induced suppression of the phonon drag, $S(T)$ reacts much more sensitively to the bombardment resulting in a purely linear behavior with negative slope for $T > 100$ K. Below 100 K, a broad peak towards even more negative values is found representing a small deviation from linearity, which is attributed to electron-phonon renormalization effects and can be described quantitatively by the corresponding theory.

I. INTRODUCTION

If a temperature gradient ∇T is established between the ends of a solid, an electric field $\mathbf{E}$ will be built up and both are related by $\mathbf{E}=S(T)\nabla T$ with $S(T)$ being the temperature-dependent absolute Seebeck coefficient or thermopower of the material under study. This long known transport phenomenon constitutes the thermoelectric effect. Its experimental observation, however, necessarily involves at least two different materials A and B with corresponding absolute coefficients S_A and S_B, respectively, forming a thermocouple. By measuring the difference of the electrical potentials ΔV_{BA} due to the temperature difference ΔT between the thermocouple, the coefficient $S_{BA}=\Delta V_{BA}/\Delta T$ can be determined, which for small ΔT is related to the individual S_A, S_B values by $S_{BA}=S_A-S_B$. Thus, to obtain the absolute value $S(T)$ of a material A, the behavior of $S_B(T)$ must be known quantitatively. In the present work, which aims at studying the temperature dependence of the Seebeck coefficient for NbN films, $S_{NbN}(T)$, lead has been chosen as material B, since the corresponding $S_{Pb}(T)$ values are known and tabulated over a wide temperature regime.[1,2]

Theoretically, based on Boltzmann transport theory it has long been shown[3] that the contribution to $S(T)$ of simple metals due to the thermal diffusion of their nearly free charge carriers exhibits a linear temperature dependence $S_{diff} \propto T$. Experimentally, in most cases this linear relationship is covered by an additional contribution S_{drag}, which is nonlinear in T and often dominating the observed $S(T)$ at least at temperatures below 300 K. This phonon drag contribution is caused by the interaction between the heat conducting phonons and the charge carriers. Its analysis is complicated by the fact that depending on whether the corresponding electron-phonon scattering is dominated by Normal (N) or Umklapp (U) processes, the drag term has to be added or subtracted from the pure diffusional contribution S_{diff}. In any case, at low temperatures $T \ll \Theta_D$ (Θ_D Debye temperature), the drag effect should freeze out reflecting the decaying probability of thermally excited phonons and at high temperatures $T \gg \Theta_D$, where phonon-phonon scattering leads to a decreasing phonon mean free path, the drag effect also should vanish. This leads to the "phonon-drag peak" mostly observed in crystalline solids. From these remarks it is clear that a quantitative description of the drag effect is complex due to the fact that besides the detailed knowledge of the electron- and phonon-dispersion relations, the interaction matrix elements have to be calculated including U processes.[4] For NbN, such a theoretical analysis is not available yet. Here, the theoretical situation is even more complicated due to the presence of a high d-band density of states, which strongly influences the scattering rate of the s electrons. Taking into account this s-d scattering, it has been shown that a nonlinear T dependence of S generally will result.[5]

For NbN also the experimental situation of $S(T)$ is not clear and different signs of S have been reported.[6–8] The present work will serve to clarify this situation. The re-

fractory materials in general and especially NbN are interesting for their superconducting properties. NbN exhibits a typical transition temperature to superconductivity T_c of up to 16.1 K, the detailed value depending on stoichiometry,[9] impurities,[10] and disorder.[11] Tunneling data in the superconducting state indicate a strong electron-phonon interaction in this conventional superconductor.[12,13] This makes NbN an attractive candidate to test the effect of electron-phonon renormalization on the Seebeck coefficient $S(T)$. Such an effect has been theoretically discussed by several authors[14–16] and experimentally demonstrated for amorphous metals.[17,18] The missing long-range order of these amorphous metals guarantees a short phonon mean free path thereby suppressing the otherwise dominating phonon-drag peak. This suppression has also been related to the high electrical resistivity of the metallic glasses.[19] This criterion, however, has to be handled with care. In the present case of NbN films, the samples exhibit electrical resistivities well above 100 $\mu\Omega$ cm, which are due to the semiconducting or even insulating behavior of the nonstoichiometric grain boundaries rather than to the structural properties of the grains themselves. As will be discussed in the present work, in such an inhomogeneous granular or columnar case, the phonon-drag peak may not be suppressed despite the high resistivity values, if the phonon mean free path l_{ph} is larger than the average grain size. In this case, without further experimental effort, the NbN films would not allow us to observe renormalization effects on $S(T)$. As will be demonstrated below, a unique tool to suppress possible drag effects in our samples is ion irradiation. By this technique, defects can be produced within the NbN grains, which are sufficient to decrease the l_{ph} low enough to suppress the drag effect, though not leading to an amorphous phase. Furthermore, since the superconducting properties of NbN are known to be quite irradiation resistant,[20] the strong electron-phonon interaction should not be significantly reduced by the ion bombardment. In this case, ion irradiation should allow to make the renormalization effects on $S(T)$ of NbN films visible. The experimental demonstration of this possibility is the main aim of the present work.

II. EXPERIMENTAL

A. Preparation and characterization of the NbN films

The NbN films were prepared by dc-magnetron sputtering from a Nb target using a Ar/N_2 plasma with a total pressure ranging between 10 and 50 mTorr resulting in a deposition rate of typical 2 nm/s. Since the determination of $S(T)$ demanded a low heat conduction along the films, they were deposited onto thin (0.1 mm) glass substrates (length 52 mm, width 12 mm) held at a temperature below 50 °C. During the deposition, part of he substrate width was covered by a mask. Thus, the resulting film dimensions were 52×7 mm^2 with total thicknesses between 150 and 400 nm. This smaller width allowed the film to be complemented by a Pb foil on the glass substrate to form a NbN/Pb thermocouple. The substrate is then glued onto a split Cu-sample holder, each side of which was equipped with a heater and a thermometer. The experimental arrangement is shown in Fig. 1, where the electrical contacts provided by small silver paint spots are indicated by dots. By this standard four-point technique the electrical resistivity of the NbN films was determined as a function of temperature $\rho(T)$ for $4.2<T<300$ K. Additionally, in this way information could be obtained on the transition temperature T_c, the temperature coefficient of the resistivity $d\rho/dT$ and the resistance ratio $r=R(300\text{ K})/R(20\text{ K})$. The NbN films of the present study exhibited residual resistivity values ranging between 350 and 600 $\mu\Omega$ cm. In all cases negative values for $d\rho/dT$ were found with corresponding resistance ratios $r<1$. Despite this combination of high ρ values and negative $d\rho/dT$, which commonly is found for amorphous metals, x-ray diffractometry clearly proved the polycrystallinity of the films. Taking the strong (111) Bragg peak together with the weaker (200) and (222) peaks, lattice parameters for the different films were obtained between 0.4386 and 0.4394 nm in close agreement with the bulk value of 0.4392 nm.[9] An average grain size of approximately 30 nm is estimated from the width of the diffraction lines. Thus, the high resistivity values have to be attributed to barriers at the grain boundaries probably due to grain-boundary oxides.[21]

The transition temperature to superconductivity of the different films varied between 13.8 and 15 K. Applying a correlation between T_c and the nitrogen stoichiometry x of NbN_x samples as given in Ref. 9, values of $x>0.84$ are obtained for our films. The above quantities for each film of the present study together with its thickness are given in Table I.

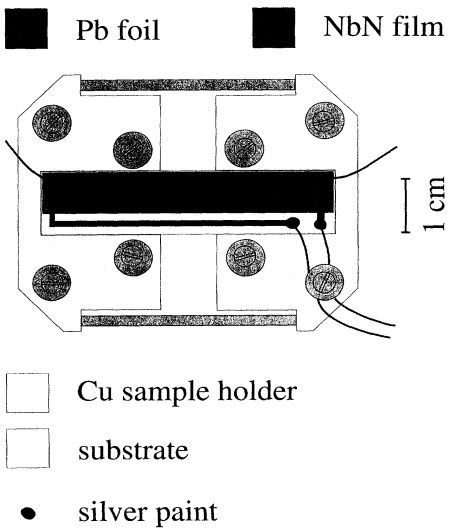

FIG. 1. Top view of the thermocouple arrangement used to measure $S(T)$.

TABLE I. Thickness d, resistivity ρ (20 K), residual resistance ratio r, transition temperature to superconductivity T_c, and nitrogen content x (from Ref. 9) of the investigated NbN_x films.

Sample	Symbol	d (nm)	ρ (20 K) ($\mu\Omega$ cm)	r	T_c (K)	x
6	■	200	369	0.89	14.95	0.88
5	♦	200	394	0.88	14.84	0.87
1	▼	400	500	0.70	14.40	0.86
3	+	150	587	0.81	14.04	0.85
4	▲	150	610	0.80	13.82	0.84
2	●	150	591	0.79	13.79	0.84

B. $S(T)$ measurement

To determine $S(T)$, a dynamic differential technique has been applied as described in detail in Ref. 22. By referring to Fig. 1, this method is briefly characterized as follows. Both halves of the Cu-sample holder can be temperature controlled separately. While ramping up the temperature of one half, the other one is kept constant. If the temperature difference ΔT developed in this way exceeds a preset upper limit ΔT_{max}, heating of that half of the holder is stopped and is switched to the other half, and so on. By this procedure, the average temperature $\bar{T}$ of the sample is increasing linearly, while the difference ΔT producing the thermoelectrical signal is oscillating in a sawtooth manner about zero. Consequently, a corresponding oscillation is found for the thermoelectric voltage ΔV. Both signals are registered simultaneously by computer controlled nanovoltmeters allowing to obtain 80 data points per heating cycle, which is attributed to one average value $\bar{T}$. From a linear fit to the ΔV versus ΔT data, the coefficient $S(\bar{T})$ is deduced. The Cu-sample holder itself is connected to the bottom of a ^{4}He cryostat allowing $S(T)$ measurements from 4.2 to 300 K. The relative errors of S were found to differ for different temperature windows. The most reliable data with $\Delta S/S < 2\%$ are obtained for $60 < T < 300$ K, the largest error with 10% is found for $30 < T < 60$ K. Details on this point are given in Ref. 8.

C. Ion irradiation

To enable the $S(T)$ measurement on ion-irradiated NbN films, the whole Cu-sample holder shown in Fig. 1 could be exposed to a beam of 350-keV Ne^+ ions with a typical current of 1 μA provided by a commercial accelerator. With an aperture mounted 2 mm above the NbN/Pb thermocouple, the irradiated area can be defined and restricted to the NbN film. The ions are horizontally and vertically scanned over this area to guarantee a homogeneous irradiation. The fluences Φ (ions per cm^2) were determined by directly integrating the ion current impinging onto the film and suppressing secondary electrons by applying a negative voltage to an additional aperture. All irradiations reported below were performed at 300 K. By exposing the whole sample holder to the beam it is possible to avoid any changes of the thermal contact between the substrate and the Cu holder provided by the glue. This turns out to be crucial to obtain meaningful data on ion-induced changes of $S(T)$.

Using Monte Carlo simulation,[23] the projected range R_p of the ions, their straggling ΔR_p as well as the total energy transferred from the ions to the target atoms by nuclear encounters (nuclear energy loss) $(dE/dx)_n$ can be calculated. In the present case of 350-keV Ne^+ irradiation of NbN, one obtains $R_p = 247$ nm, $\Delta R_p = 75$ nm, and an average value of $(dE/dx)_n$ taken at $x = d/2$ of 271 eV/nm. Comparison of these range data to the typical film thickness of 200 nm indicates that most of the ions ($> 90\%$) penetrate the film thereby producing radiation damage. Quantitatively, the damage due to the bombardment with an ion fluence Φ commonly is described by the average number of displaced target atoms (dpa), which can be approximated by $\text{dpa} = \Phi \cdot (dE/dx)_n / (2E_d N)$ with the number density of the target N and the average displacement threshold energy E_d.

III. RESULTS AND DISCUSSION

A. Unirradiated NbN films

Following recent work by Morelli,[24] who analyzed his $S(T)$ data on TiC_x crystals in terms of the s-d-scattering model,[5] in Fig. 2 a similar analysis is presented for two NbN_x films with $x = 0.92$ (crosses, same data as in Ref. 8) and $x = 0.86$ (triangles). In this figure, only every third point of the actually taken data is plotted for clarity. The experimental results exhibit positive $S(T)$ values for all $T < T_{max} = 300$ K with a broad maximum at about 110 K. For the film with smaller x, the maximum is more pronounced with its values of S below the corresponding ones of the more stoichiometric sample. As will be shown below, this trend is continued for even smaller x (cf. Fig. 3) and for the most understoichiometric film with $x = 0.84$ a sign change of $S(T)$ is observed at 250 K.

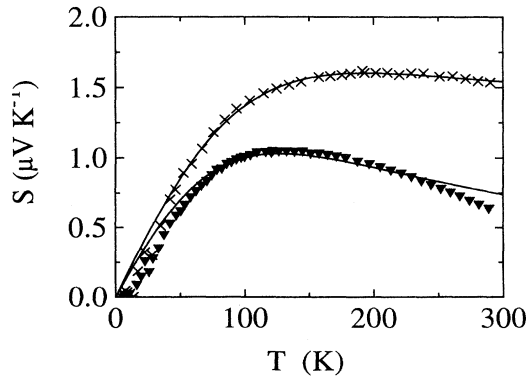

FIG. 2. $S(T)$ for two NbN_x films with $x = 0.92$ (crosses, data from Ref. 8) and $x = 0.86$ (triangles). The solid lines are fits of Eq. (4) to the data, the resulting parameters are given in Table II.

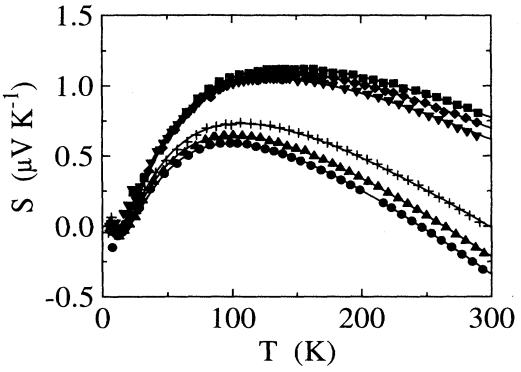

FIG. 3. $S(T)$ for NbN_x films with different x values. The symbols and x values are given in Table I. The solid lines are fits of Eq. (8) to the data, the resulting parameters are given in Table III.

Above this temperature, the film exhibits negative S values.

In the s-d model by Lye,[5] the total Seebeck coefficient can be expressed as

$$S=\frac{AT}{1+(A/B)[T_m T^2/(T^2+T_m^2)]} . \tag{1}$$

Here, the diffusional part is given by $S_{\text{diff}}=AT$. The coefficients T_m and B are related to higher-energy derivations $d^{(n)}\sigma(E)/dE^{(n)}$ of the electrical conductivity $\sigma(E)$ in the following way

$$B=\frac{2\pi k_B}{e}\left[\frac{\sigma'''}{6\sigma'}\right]^{1/2}\left[\frac{\sigma''}{\sigma'}-\frac{\sigma\sigma'''}{(\sigma')^2}\right]^{-1};$$
$$T_m=\frac{1}{\pi k_B}\left[\frac{6\sigma'}{\sigma'''}\right]^{1/2} . \tag{2}$$

Introducing

$$C\equiv B^{-1}T_m^{-1}=\frac{e}{2}\left[\frac{\sigma''}{\sigma'}-\frac{\sigma\sigma'''}{(\sigma')^2}\right] \tag{3}$$

results in

$$S=\frac{AT}{1+AC[T_m^2 T^2/(T^2+T_m^2)]} . \tag{4}$$

This expression has been fitted to the data of Fig. 2 with A, C, and T_m as fitting parameters. The results are included in Fig. 2 as solid lines, the corresponding parameters are summarized in Table II.

These results show that the most stoichiometric $NbN_{0.92}$ film can be well described by the s-d model, though there are significant deviations at $T<50$ K. For the more understoichiometric $NbN_{0.86}$, however, clear deviations of the experimental data from the fit are found below 80 and above 220 K. Furthermore, while the absolute values of the fit parameters obtained for the $NbN_{0.92}$ film compare quite well with the corresponding results obtained for $TiC_{0.88}$ crystals,[24] the parameter T_m has to be set infinite [as a consequence, according to Eq. (3) $B=0$ or, equivalently, due to Eq. (2) $\sigma'''=0$]. On the other hand, for a given set of A, C, and T_m, the general form of Eq. (4) implies that a sign change of $S(T)$ either is impossible or it occurs at an unphysical discontinuous singularity. Since, however, such a sign change is observed experimentally for films with $x\leq 0.85$, the s-d model is not appropriate in these cases. As will be demonstrated now, the assumption of a significant phonon-drag effect allows to describe the data of films with different x values in a consistent manner. A necessary condition for such an assumption is a sufficiently large value of l_{ph}. Unfortunately, since experimental thermal conductivity data are not available for NbN, l_{ph} has to be estimated from theoretical approximations for the phonon-phonon scattering time as given, e.g., in Ref. 4, p. 128. Here, the most important input parameters are the Debye temperature, the velocity of sound, and the Grüneisen parameter. In view of the uncertainty of the input parameters, the resulting value of l_{ph} (300 K)=40 nm mainly due to the high value of $\Theta_D=600$ K, can only be taken as a rough order of magnitude estimate, which is compatible with the idea of a phonon-drag effect. In Fig. 3, the $S(T)$ data for all films characterized in Table I are presented. As already mentioned above, the data clearly demonstrate the existence of a sign change from positive to negative values within the observed temperature range for $x\leq 0.85$ (for larger x, these changes only can be extrapolated), and the trend that the more understoichiometric (smaller x) films exhibit lower $S(T)$ values.

TABLE II. Parameters obtained by fitting Eq. (4) to the $S(T)$ data of two NbN_x films.

Sample	x	T_c (K)	A (μV/K^2)	B (μV/K)	C (μV^{-1})	T_m (K)
Ref. 8	0.92	16.1	0.0186	0.877	3.834×10^{-3}	570
1	0.86	14.4	0.0162	0	3.818×10^{-3}	∞

If the overall behavior of $S(T)$ as presented in Fig. 3 is to be interpreted in terms of the phonon-drag effect, one has to assume a negative diffusional thermopower S_{diff}, the linear T dependence of which is approached at high temperatures, and a phonon-drag contribution of opposite sign dominating at about 100 K. This opposite sign necessarily demands the dominance of U processes for the drag effect. Thus, the total $S(T)$ is assumed as composed of three contributions

$$S(T)=S_{\text{diff}}+S_{\text{drag}}^N+S_{\text{drag}}^U . \tag{5}$$

Here, S_{drag}^N and S_{drag}^U indicate the Normal and Umklapp contribution to the phonon-drag thermopower, respectively. Following MacDonald, Pearson, and Templeton,[25] the U part can be described by

$$S_{\text{drag}}^U \propto \exp\left[-\frac{\Theta^*}{T}\right] \tag{6}$$

with Θ^* being a characteristic temperature ranging be-

tween $\Theta_D/10$ and $\Theta_D/5$.

Assuming the standard form for the N part, i.e., $S^N_{\text{drag}} \propto T^3$,[4] and combining with Eqs. (5) and (6), results in the expression

$$S(T) = AT + BT^3 + C \exp\left[-\frac{\Theta^*}{T}\right]. \quad (7)$$

This expression has been least-squares fitted in the data of Fig. 3 with A, B, C, and Θ^* as fit parameters obeying in the present case the additional conditions $A, B \leq 0$ and $C, \Theta^* \geq 0$. In practice, it turned out that the best fits were obtained with $B = 0$ for all films. The corresponding results are given as solid lines in Fig. 3, the numerical values of the parameters are summarized in Table III. As can be seen, the experimental $S(T)$ behavior of the different NbN_x films is excellently described by Eq. (7) for all the x values studied. Among the extracted parameters, the slope A of the diffusional part appears to be the most sensitive to changes of x, while C and Θ^* exhibit a decrease due to smaller x values of only 15% and 5%, respectively. $B = 0$ indicates that N processes can be neglected for all x. In Ref. 8, a Debye temperature of 750 K has been calculated from an experimentally determined phonon density of states. Thus, the Θ^* values given in Table III are of the order $\Theta_D/13$ close to what is expected empirically. These values also justify the application of Eq. (6), which only should hold for $T \ll \Theta_D$.

The excellent description of the experimental $S(T)$ data for NbN_x films with different x values by Eq. (7) as demonstrated in Fig. 3, suggests that a phonon-drag effect dominated by U processes is governing the Seebeck coefficient within its positive range of data despite the high resistivities of the samples. In our opinion, this conclusion is not in conflict with the general idea of a phonon-drag suppression in strongly disordered homogeneous samples. It rather reflects the inhomogeneity of our NbN films due to their granular or columnar structure with many grain boundaries dominating the total electrical resistance. It should be noted, however, that Eq. (7) for temperatures $T \gg \Theta^*$, delivers a constant offset given by the coefficient C. This offset is needed to describe the experimental data, but it is not consistent with an exclusively acting phonon-drag effect. In this case, at high temperatures the effect is expected to die out like $\sim 1/T$. The physical origin of this additional offset is not known at present.

For higher temperatures, $S(T)$ approaches its linear diffusional regime with a corresponding negative slope. The fact that the crossover temperature for this sign change strongly depends on x, may explain why for NbN bulk samples different signs of $S(300\ \text{K})$ have been reported. It is interesting that the overall behavior of $S(T)$ of the more understoichiometric NbN samples closely resembles the result found for pure Nb,[26] with a broad positive phonon-drag peak extending up to 250 K accompanied by a crossover to negative values at this temperature. Another point appears worth noting in this context. For high-resistivity samples a thermopower analog to the Mooij correlation has been reported[27] indicating an increase of thermopower magnitude $|S|$ as the square of resistivity. The present experimental data seem to contradict this correlation due to the observed sign change of S observed for the films with higher resistivities. If, however, the diffusional part $S_{\text{diff}}(300)$ as calculated with the parameters A from Table III, is plotted versus $\rho(20)$ as given in Table I, an approximately quadratic correlation is found. This, indirectly, corroborates the negative sign of the diffusion thermopower of NbN films in contrast to the conclusion drawn in Ref. 8.

If the above conclusion concerning the dominance of the phonon-drag effect holds true, it should be possible to obtain the pure diffusional part of $S(T)$ by its suppression. A way to realize this idea is to introduce disorder within the NbN grains thereby reducing the phonon mean free path. Experimentally, this can be accomplished by ion irradiation resulting in the production of lattice defects. The results of such experiments, which provide a crucial test of the above phonon-drag assumption, will be presented in the following.

TABLE III. Parameters obtained by fitting Eq. (7) to the experimental data for different NbN_x films.

Symbol	x	A (nV K^{-2})	C (μ V K^{-1})	Θ^* (K)
■	0.88	−4.93±0.08	2.72±0.03	56.1±0.5
♦	0.87	−5.12±0.06	2.69±0.02	55.6±0.4
▼	0.86	−5.07±0.05	2.54±0.02	51.4±0.3
+	0.85	−6.61±0.05	2.35±0.02	52.7±0.3
▲	0.84	−7.70±0.05	2.37±0.02	56.0±0.4
●	0.84	−7.22±0.05	2.33±0.02	53.7±0.4

B. Ion-irradiated NbN films

Ion bombardment of NbN_x films at $T_{\text{irr}} = 300$ K with 350-keV Ne^+, in all cases resulted in a resistivity enhancement. An example of this behavior is shown in Fig. 4, where the temperature dependence of the resistivity $\rho(T)$ of film No. 3 (cf. Table I) is presented as obtained

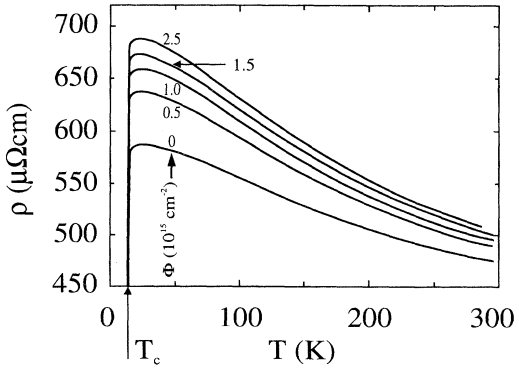

FIG. 4. Electrical resistivity ρ as a function of temperature T for the NbN film No. 3 (cf. Table I) after ion irradiation at $T_{\text{irr}} = 300$ K (350-keV Ne^+) with fluences ϕ as assigned to each curve.

after ion irradiation with different fluences Φ. Clearly, the irradiated film exhibits larger absolute values of the negative temperature coefficients accompanied by decreasing residual resistance ratios r for increasing fluences. This means that the effect of the bombardment on ρ cannot be described by Matthiessen's rule, which assumes a temperature independent resistivity enhancement $\Delta\rho(\Phi)$. It rather points to an ion induced change of the electron-phonon coupling.

At a fixed temperature $T < T_{irr}$, the corresponding resistivity enhancement $\Delta\rho(\Phi, T, T_{irr})$ shows a saturation behavior, which can be characterized by the function

$$\Delta\rho(\Phi) = a[1 - \exp(-b\Phi)] . \quad (8)$$

An example of this behavior is given in Fig. 5(a), where the quantity $\rho_{273}(\Phi) = \rho(\Phi = 0) + \Delta\rho(\Phi, 273, 300)$ is presented together with a fit to Eq. (8) for film No. 3. This result is similar to what has been reported for the effect of 200-keV Ar^+ irradiation at 300 K on NbN films.[20] It turns out that the fit parameter b in Eq. (8) is temperature independent, i.e., for a given film and fixed T_{irr} the ion-induced enhancement can be written as

$$\Delta\rho(\Phi, T, T_{irr}) = \Delta\rho_{sat}(T)[1 - \exp(-b\Phi)] . \quad (9)$$

The saturation values $\Delta\rho_{sat}$ obtained at 273 K due to the Ne^+ irradiations are relatively small (of the order of 5%) in agreement with previous results[20] confirming the good radiation resistance of NbN.

This insensitivity against ion bombardment is also found for the correspondence changes of the transition temperature to superconductivity as can be seen from Fig. 5(b), where T_c of film No. 3 is plotted versus the Ne^+ fluence. The solid line is a fit to Eq. (8) with $\Delta\rho(\Phi)$ substituted by $\Delta T_c(\Phi)$. A T_c decrease by 14% is obtained in this way comparable to previous results.[20,28].

In contrast to the resistivity and T_c, the Seebeck coefficient and its temperature dependence is strongly influenced by the ion bombardment. This is demonstrated in Figs. 6(a) and 6(b) for two NbN_x films of comparable stoichiometry, but significantly different thicknesses (films 1 and 3, cf. Table I). By this choice, since in case of the thick film in Fig. 6(b) practically all Ne atoms are implanted within the sample, while in case of the much thinner film shown in Fig. 6(a) most of the ions penetrate the sample, it can be tested whether there are additional effects due to Ne implantation. The experimental results shown in Fig. 6 suggest that such effects can be neglected. The most prominent feature of these irradiation results is a parallel shift of the linear high-temperature part of $S(T)$ towards negative values accompanied by a gradual disappearance of the phonon-drag peak. Eventually, for the highest fluences $S(T)$ exhibits a purely diffusional behavior above 100 K with a totally suppressed drag peak and a negative slope extrapolating to zero [dashed lines in Figs. 6 (a) and 6(b)]. This result confirms the idea discussed above that the ion-induced defects within the

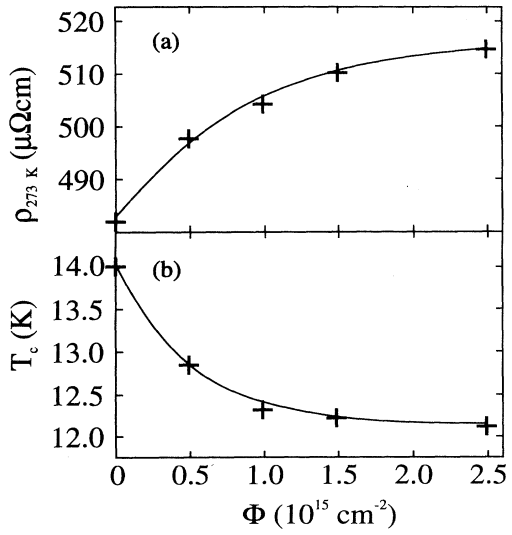

FIG. 5. (a) Ion-induced resistivity changes of film No. 3 observed at 273 K after ion irradiation at $T_{irr} = 300$ K (350-keV Ne^+) with fluences ϕ. The solid line is a fit to Eq. (9). (b) Ion-induced changes of the transition temperature to superconductivity T_c corresponding to (a). The solid line is a fit to Eq. (9).

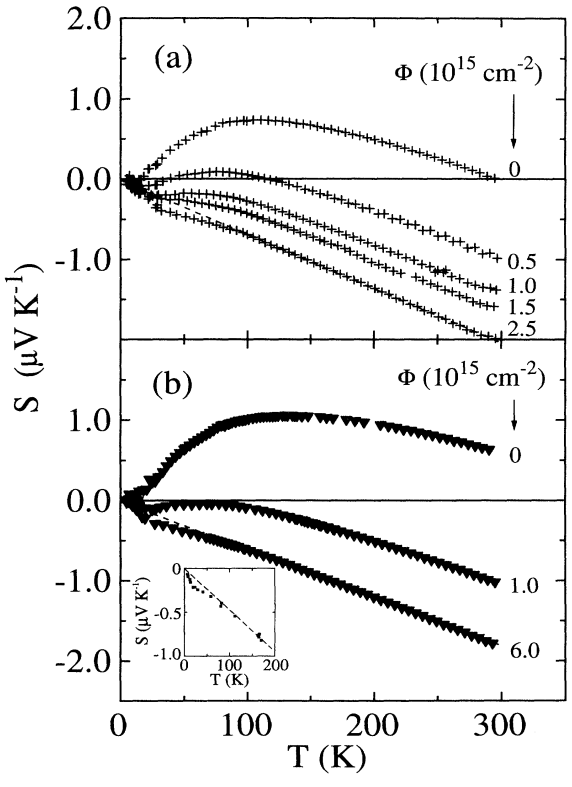

FIG. 6. Ion-induced changes of the thermopower $S(T)$ of (a) film No. 3 (thin film) after ion irradiation at $T_{irr} = 300$ K (350-keV Ne^+) with fluences ϕ as assigned to each curve. (b) film No. 1 (thick film) after ion implantation at $T_{irr} = 300$ K (350-keV Ne^+) with fluences ϕ as assigned to each curve. The insert shows $S(T)$ data obtained for amorphous $La_{0.78}Ga_{0.22}$ (Ref. 28).

grains lead to a strongly reduced phonon mean free path resulting in the suppression of the drag effect. Furthermore, the data indicate that the above addressed constant offset of $S(T)$ at high temperatures, is continuously reduced by the ion bombardment in parallel to the drag effect until, at high fluences, this offset becomes zero as demonstrated by the extrapolating dashed lines in Fig. 6. Since in general, defects tend to smear out characteristic features of electronic bands, one may take the above behavior of $S(T)$ offset as a hint that a characteristic Fermi surface topology is necessary for its existence, which is washed out by ion irradiation. In this context, Eq. (7) emphasizes the role of U processes as contributing to both, the phonon drag part of $S(T)$ and its offset.

The small deviation from the linear behavior of $S(T)$ below 100 K towards more negative values, closely resembles to what has been observed for amorphous metals. To demonstrate this similarity, the inset of Fig. 6(b) shows corresponding results obtained for amorphous $La_{0.78}Ga_{0.22}$.[29] In this case, the deviation from linearity has been attributed to an electron-phonon renormalization effect and a similar analysis will be given below.

Quite generally, the Seebeck coefficient S_m of a binary mixture consisting of materials A and B with coefficients S_A, S_B can be calculated, if the electrical conductivities σ_A, σ_B of the pure materials and σ_m of the mixture are known and if the corresponding thermal conductivities κ_A, κ_B, and κ_m are approximately equal.[30] It is worth noting that by formally taking the unirradiated state of the NbN_x films as material A and their final state after irradiation with the highest fluence as material B, $S(T)$ for the intermediate fluences could be calculated from the corresponding measured resistivity data without any fitting parameter and excellent agreement has been found with theory.[31] In the light of the present paper, the physical interpretation of A and B becomes more clear. The irradiated films can be modeled as consisting of two types of grains, one with a low density of defects and, correspondingly, with l_{ph} still larger than the grain size, the other with a high density of defects and l_{ph} smaller than this size. As a consequence, in type one grains the phonon drag as well as the $S(T)$ offset is still present, while in type two grains both are totally suppressed. If all grains have been transformed into type two by the ion bombardment, the final state B is obtained.

As has been shown in Refs. 15 and 16, the metallic diffusion thermopower in the presence of electron-phonon interaction can be written in the form

$$S(T)=[1+\lambda(T)]S^b_{\rm diff}(T)+[2\alpha+\gamma]\lambda(T)T \ . \qquad (10)$$

Here, $S^b_{\rm diff}$ is the bare diffusion thermopower in the absence of the electron-phonon interaction, i.e., $S^b_{\rm diff}=AT$ as above. The electron-phonon enhancement factor is expressed by $\lambda(T)$, which, in the limit $T=0$, is identical with the standard mass enhancement factor λ_0 due to this interaction as can be seen from

$$\lambda(T)=2\int_0^\infty \frac{\alpha^2F(\omega)}{\omega} G\left[\frac{\hbar\omega}{k_BT}\right] d\omega \ , \qquad (11)$$

where $\alpha^2F(\omega)$ is the Eliashberg function containing all information on the electron-phonon coupling and $G(\hbar\omega/k_BT)$ is a function derived and evaluated in Ref. 15 with $G(\infty)=1$ and $G(0)=0$. The quantity α in Eq. (10) describes the effect of velocity and relaxation time renormalization, while γ gives the contribution from higher-order diagrams (Nielsen-Taylor effect). To a first approximation[15,16], α and γ exhibit the same temperature dependence as $\lambda(T)$, i.e., they can be taken as constants in Eq. (10). With the normalized quantity $\bar{\lambda}=\lambda(T)/\lambda_0$, Eq. (10) can be rewritten as

$$S(T)=AT+c\bar{\lambda}(T)T \quad \text{with } c=\lambda_0(A+2\alpha+\gamma) \ . \qquad (12)$$

This expression has been fitted to the experimental $S(T)$ data obtained for NbN films irradiated with the highest ion fluences. An example of this procedure is given in Fig. 7 for film No. 1 after ion irradiation with a fluence of 6×10^{15} cm^{-2}. From a fit to Eq. (12) given by the solid curve in the figure, the following parameters were extracted: $A=-5.94$ nV K^{-2} and $c=-7.26$ nV K^{-2}. Implicit in this fitting procedure is an assumption on the form of $\alpha^2F(\omega)$, which is needed to calculate $\lambda(T)$ according to Eq. (11). In contrast to Ref. 8, where a model $\alpha^2F(\omega)$ has been used based on experimental tunneling and neutron-scattering results, for irradiated NbN films such data are not available. Thus, a simple Debye-like power-law approximation was adopted of the form $\alpha^2F(\omega)=B\omega^2$ with an upper cutoff frequency ω^* as a further fit parameter (the numerical value of the proportionality constant B is not needed since it drops out by using the normalized quantity $\bar{\lambda}$). Expressing ω^* by an equivalent temperature Θ^*, in the above case of Fig. 7, $\Theta^*=90$ K is obtained, i.e., a small value compared to the Debye-temperature Θ_D. This can be understood referring to Eq. (11), which indicates that all phonon frequencies are weighted by $1/\omega$ in calculating $\lambda(T)$. As a consequence, the main contribution stems from the acoustic

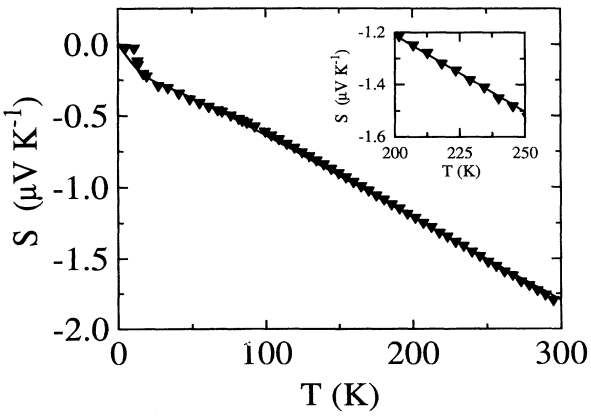

FIG. 7. $S(T)$ behavior after ion irradiation of film No. 1 at $T_{\rm irr}=300$ K (350-keV Ne^+) with a fluence $\phi=6\times10^{15}$ cm^{-2}. The solid line is a fit to Eq. (13), which describes the effect electron-phonon renormalization. To make the fitted line more visible, an expanded view is given in the insert.

phonons and even if the optical phonons are totally cut off by restricting $\hbar\omega$ to below 40 meV, the corresponding λ_0 is decreased by only 21%. For the calculation of Θ_D, however, the optical phonons, which extend up to approximately 85 meV in NbN,[8] and the acoustic phonons have to be handled on equal footing.

With $\lambda_0=1.19$ from Ref. 8 and A as numerically given above, Eq. (12) delivers for the magnitude of $(2\alpha+\gamma)$ a value of 0.16 nV K^{-2}, which is much smaller than A indicating that the renormalization of the velocity and relaxation time as well as higher-order terms play only a minor role compared to energy renormalization. The theoretical description of this latter effect, however, is in excellent agreement with the experimental results.

In summary, the present study has provided experimental evidence that the thermopower of NbN_x films and its temperature behavior depend on stoichiometry x. The overall behavior of $S(T)$ could be quantitatively analyzed in terms of a superposition of a positive phonon-drag contribution, a constant offset and a linear diffusional thermopower with a negative slope. Furthermore, it could demonstrated for the first time that ion irradiation can be applied to systematically reduce the phonon mean free path until the phonon-drag effect is totally suppressed together with the $S(T)$ offset. The final linear diffusion thermopower obtained in this way, still exhibits small deviations from linearity below 100 K, which can be explained as being due to electron-phonon renormalization and described very well by the corresponding theory.

ACKNOWLEDGMENTS

We would like to thank Dr. H. Downar (Dornier GmbH) for growing the NbN films, A. Plewnia for experimental support during the ion bombardments, and Th. Theilig for his assistance.

[1]R. B. Roberts, Philos. Mag. **36**, 91 (1977).
[2]R. B. Roberts, Philos. Mag. B **43**, 1125 (1981).
[3]N. F. Mott, Proc. R. Soc. London Ser. A **153**, 699 (1936).
[4]R. D. Barnard, *Thermoelectricity in Metals and Alloys* (Taylor & Francis, London, 1972).
[5]R. G. Lye, J. Phys. Chem. Solids **26**, 407 (1965).
[6]T. S. Verkhoglyadova, S. N. L'vov, V. F. Nemchenko, and G. V. Samsonov, Sov. Phys. J. **10/8**, 17 (1967).
[7]S. N. L'vov, V. F. Nemchenko, and G. V. Samsonov, Sov. Phys. Dok. **135**, 1334 (1960).
[8]S. Reiff, R. Huber, P. Ziemann, and A. B. Kaiser, J. Phys. Condens. Matter **1**, 10 107 (1989).
[9]G. Brauer and H. Kirner, Z. Anorg. Allg. Chem. **328**, 34 (1964).
[10]I. Hotovy and J. Huran, Phys. Status Solidi A **137**, K25 (1993).
[11]H. W. Weber, P. Gregshammer, K. E. Gray, and R. T. Kampwirth, IEEE Trans. Magn. **25**, 2080 (1989).
[12]J. Geerk, U. Schneider, W. Bangert, H. Rietschel, F. Gompf, M. Gurvitch, J. Remeika, and J. Rowell, Physica B **135**, 187 (1985).
[13]K. E. Kihlstrom, R. W. Simon, and S. A. Wolf, Phys. Rev. B **32**, 1843 (1985).
[14]J. L. Opsal, B. J. Thaler, and J. Bass, Phys. Rev. Lett. **36**, 1211 (1976).
[15]A. B. Kaiser, J. Phys. F **12**, L223 (1982); Phys. Rev. B **29**, 7088 (1984).
[16]A. B. Kaiser and G. E. Stedman, Solid State Commun. **54**, 91 (1985).
[17]H. Armbrüster and D. G. Naugle, Solid State Commun. **39**, 675 (1981).
[18]C. Lauinger, J. Feld, E. Compans, P. Häussler, and F. Baumann, Physica B **165&166**, 289 (1990).
[19]J. Jäckle, J. Phys. F **10**, L43 (1980).
[20]J. Y. Juang, D. A. Rudman, J. Talvacchio, and R. B. van Dover, Phys. Rev. B **38**, 2354 (1988).
[21]A. Darlinski and J. Halbritter, Surf. Interface Anal. **10**, 223 (1987).
[22]E. Compans, Rev. Sci. Instrum. **60**, 2715 (1989).
[23]J. F. Ziegler, J. P. Biersack, and U. Littmark, *The Stopping and Range of Ions in Solids* (Pergamon, New York, 1985), Vol. 1.
[24]D. T. Morelli, Phys. Rev. B **44**, 5453 (1991).
[25]D. K. C. Macdonald, W. B. Pearson, and I. M. Templeton, Proc. R. Soc. London, Ser. A **256**, 334 (1960).
[26]R. Carter, A. Davidson, and P. A. Schroeder, J. Phys. Chem. Solids **31**, 2374 (1970).
[27]A. B. Kaiser, Phys. Rev. B **35**, 2480 (1987).
[28]V. Jung, in *Proceedings of the 17th International Conference on Low Temperature Physics,* edited by U. Eckern, A. Schmid, W. Weber, H. Wühl (Elsevier Science, Amsterdam, 1984), p. 109.
[29]H. Armbrüster and D. G. Naugle, Solid State Commun. **39**, 675 (1981).
[30]V. Halpern, J. Phys. C **16**, L217 (1983).
[31]The. Siebold and P. Ziemann, Solid State Commun. **87**, 269 (1993).

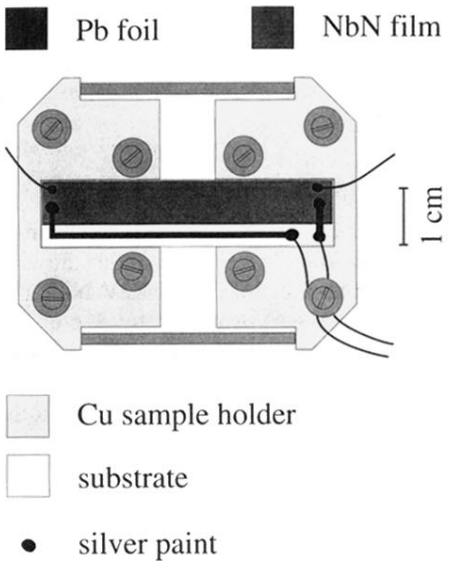

FIG. 1. Top view of the thermocouple arrangement used to measure $S(T)$.